

Topologically Unique Heterometallic Cu^{II}/Li Coordination Polymers Self-Assembled from *N,N*-bis(2-Hydroxyethyl)-2-aminoethanesulfonic Acid Biobuffer: Versatile Catalyst Precursors for Mild Hydrocarboxylation of Alkanes to Carboxylic Acids

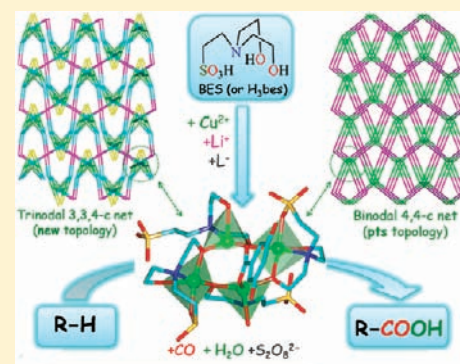
Marina V. Kirillova,[†] Alexander M. Kirillov,^{*,†} André N. C. Martins,[†] Claudia Graiff,[‡] Antonio Tiripichio,[‡] and Armando J. L. Pombeiro^{*,†}

[†]Centro de Química Estrutural, Complexo I, Instituto Superior Técnico, Technical University of Lisbon, Av. Rovisco Pais, 1049–001 Lisbon, Portugal

[‡]Dipartimento di Chimica Generale ed Inorganica, Chimica Analitica, Chimica Fisica, Università di Parma, Viale delle Scienze 17/A, I-43100, Parma, Italy

S Supporting Information

ABSTRACT: The facile aqueous medium reactions of copper(II) nitrate with BES biobuffer [(HOCH₂CH₂)₂N(CH₂CH₂SO₃H), hereinafter referred as H₃bes] in the presence of various benzenecarboxylic acids [benzoic (Hba), 3-hydroxybenzoic (Hhba), and 3,5-dihydroxybenzoic (Hdhba) acid] and lithium hydroxide gave rise to the self-assembly generation of three new heterometallic Cu^{II}/Li materials, [Li(H₂O)₄][Cu₄(μ₂-Hbes)₄(μ₂-ba)]·H₂O (**1**) and [Cu₄(μ₃-Hbes)₄(L){Li(H₂O)₂}]_n·3nH₂O {L = μ₂-hba (**2**) and μ₂-dhba (**3**)}. They were isolated as air-stable crystalline solids and fully characterized by infrared (IR) and UV–vis spectroscopy and electrospray ionization (ESI)-MS(±), elemental, thermal, and single-crystal X-ray diffraction analyses. The latter revealed that **1**–**3** have comparable packing patterns and unit cell parameters, being composed of similar [Cu₄(μ-Hbes)₄(μ-carboxylate)][−] cores and [Li(H₂O)₄]⁺ cations (in **1**) or [μ-Li(H₂O)₂]⁺ groups (in **2** and **3**), which are arranged into discrete 0D aggregates in **1** or infinite 3D noninterpenetrating metal–organic networks in **2** and **3**. The topological analysis of the coordination polymers **2** and **3** disclosed the trinodal 3,3,4-connected underlying nets with an unprecedented topology defined by the point symbol of (4.6.8)₄(4².6)₂(6².16².18²), further simplification of which resulted in the binodal 4,4-connected nets with the pts (PtS) topology. Apart from representing very rare examples of coordination compounds derived from H₃bes, **1**–**3** feature solubility in water and were applied as efficient and versatile catalyst precursors for the mild (60 °C) single-pot hydrocarboxylation, by CO and H₂O, of various gaseous, linear, and cyclic C_n (n = 2–9) alkanes into the corresponding C_{n+1} carboxylic acids, in H₂O/MeCN medium under homogeneous conditions and in the presence of potassium peroxodisulfate. Total yields (based on alkane) of carboxylic acids up to 78% were achieved, which are remarkable in the field of alkane functionalization under mild conditions, especially for a C–C bond formation reaction in aqueous acid-solvent-free medium.



INTRODUCTION

The design of coordination polymers (CPs) is nowadays a hot research topic that spreads along diverse areas of chemical science, with particular emphasis on crystal engineering, inorganic, coordination, supramolecular, and materials chemistry.^{1,2} The increased interest in CPs is governed by the structural versatility and the constantly growing diversity of applications for such materials. The search for new organic building blocks to construct metal–organic networks with desired functional properties is also a challenging field of research, since the introduction of a certain type of organic node or linker can affect the structural, topological, and physicochemical characteristics of CPs.^{1,2}

Although a number of synthesized CPs has witnessed a vast growth in recent years,^{3,4} there are still only limited examples of

such compounds that feature solubility in water^{5,6} or find applications in aqueous phase catalytic transformations.^{5b–d,7} Besides, at least a partial hydrosolubility of CPs is a desirable characteristic for their potential biological and medical applications.⁸ Bearing all these points in mind, we have focused our attention on some aqua-soluble, commercially available, and nontoxic biological buffers, the use of which as *N,O*-building blocks in the design of metal–organic networks remains underexplored. Hence, in our prior studies,^{5b,d,9} we have shown that common biobuffers, namely, TEA [triethanolamine], BIS-TRIS [bis(2-hydroxyethyl)amino-tris-(hydroxymethyl)methane], and BES [*N,N*-bis(2-hydroxyethyl-

Received: January 17, 2012

Published: April 6, 2012

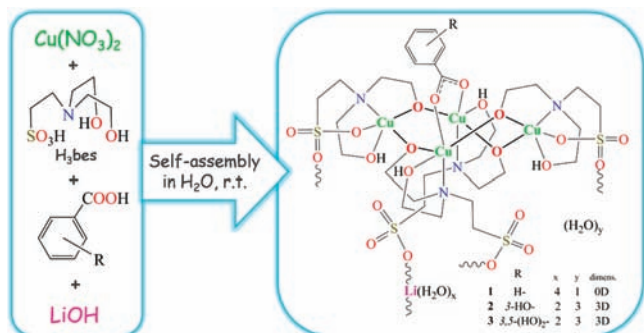
yl)-2-aminoethanesulfonic acid, hereinafter H₃bes], can act as versatile multidentate ligands for the self-assembly generation of coordination or supramolecular networks composed of multicopper(II) cores which, apart from possessing hydro-solubility, have also found a noteworthy application in the oxidation catalysis.

To further extend both of these synthetic and catalytic directions, the current work aims at the self-assembly synthesis of new hydrosoluble heterometallic coordination polymers driven by H₃bes and their application in the mild hydro-carboxylation of alkanes as bioinspired catalyst precursors relevant to particulate methane monooxygenase (pMMO).¹⁰ The choice of H₃bes is explained by its very poorly explored coordination chemistry^{4,5b} in spite of the potential to act as a versatile tetradentate N,O₃-ligand with different O-functional groups (OH, SO₃H). Hence, we report herein a facile route for three new heterometallic Cu^{II}/Li materials, namely, the discrete 0D complex [Li(H₂O)₄][Cu₄(μ₂-Hbes)₄(μ₂-ba)]·H₂O (**1**) and the infinite 3D metal–organic networks [Cu₄(μ₃-Hbes)₄(L)-{Li(H₂O)₂}]_n·3nH₂O {L = μ₂-hba (**2**) and μ₂-dhba (**3**)}, which are readily formed by self-assembly of simple chemicals in aqueous medium. The obtained compounds have been fully characterized by including single-crystal X-ray diffraction analyses, which also allowed the identification of an undocumented topology in the underlying networks of **2** and **3**. All the compounds **1–3** not only constitute very rare examples of H₃bes metal derivatives but also feature solubility in water and act as efficient and versatile catalyst precursors for the mild (60 °C) single-pot hydrocarboxylation, by CO and H₂O, of various gaseous, linear, and cyclic C_n (n = 2–9) alkanes into the corresponding C_{n+1} carboxylic acids.

RESULTS AND DISCUSSION

Synthesis and Characterization. In recent years, we have developed a versatile self-assembly synthetic procedure in

Scheme 1. Aqueous Medium Self-Assembly Synthesis and General Structural Formula of Compounds 1–3^a



^aPolymeric extensions depicted for simplicity by the squiggly line concern only compounds **2** and **3**.

aqueous medium^{5b–d,9} for the generation of diverse multicopper(II) complexes, 1D and 2D coordination polymers, as well as 3D metal–organic networks. The extension of this procedure to heterometallic Cu^{II}/Li compounds driven by H₃bes biobuffer has been attempted in the present work. Thus, the combination in water, in air, and at 25 °C, of copper(II) nitrate as a metal source with H₃bes as a main ligand source and spacer, followed by the alkalization of the obtained reaction mixture with lithium hydroxide (pH-regulator) and the addition

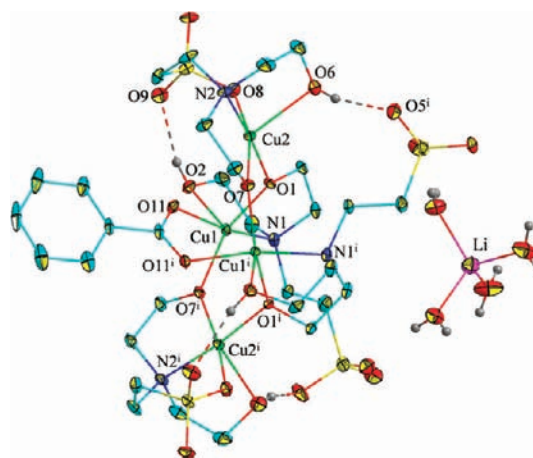


Figure 1. Crystal structure of **1** with a partial atom labeling scheme. Displacement ellipsoids are drawn at the 30% probability level. H atoms (apart from those of OH and H₂O moieties) and the crystallization water molecule are omitted for clarity. Intramolecular O2–H2...O9 [2.835(6) Å, 167.8(7)°] and O6–H6...O5ⁱ [2.704(5) Å, 164.5(7)°] hydrogen bonds are shown as dotted lines. For symmetry code, see Table 1.

of the corresponding benzenecarboxylic acid (Hba, Hhba, or Hdhba for **1–3**, respectively) as an ancillary ligand source, results in the self-assembly formation of the discrete (0D) complex [Li(H₂O)₄][Cu₄(μ₂-Hbes)₄(μ₂-ba)]·H₂O (**1**), and the structurally related 3D heterometallic Cu^{II}/Li coordination polymers [Cu₄(μ₃-Hbes)₄(μ₂-hba){Li(H₂O)₂}]_n·3nH₂O (**2**) and [Cu₄(μ₃-Hbes)₄(μ₂-dhba){Li(H₂O)₂}]_n·3nH₂O (**3**) (Scheme 1). In comparison to **1**, the main distinctive feature of **2** and **3** arises from the different μ₃-bridging mode of tetra- and pentadentate Hbes ligands, owing to the additional binding of sulfonate groups to lithium atoms. A key role in defining the dimensionality of the obtained compounds is played by the type of ancillary benzenecarboxylate ligand. The new products **1–3** have been isolated as turquoise air-stable crystalline solids in good yields (~70% based on Cu^{II} nitrate) and fully characterized by infrared (IR) and UV–vis spectroscopy and electrospray ionization (ESI)-MS(±), elemental, thermal, and single-crystal X-ray diffraction analyses.

The compounds **1–3** display solubility in water (S_{25°C} ≈ 5–6 mg mL⁻¹). This feature is of particular significance for the polymers **2** and **3**, since hydrosoluble CPs are still rare⁵ and possess a high potential^{5a,8} for biological or catalytic applications in aqueous media. In H₂O solution, **2** and **3** eventually dissociate into ionic species upon decoordination of carboxylate ligands, as confirmed by ESI-MS(±) spectra.

The ESI-MS(+) plots of aqueous solutions of **1–3** exhibit related fragmentation patterns, albeit being slightly different in relative intensity. For example, the intensity of the parent [Cu₄(Hbes)₄Li]⁺ (m/z = 1105) fragment ranges from 40% in **1** to 70 and 100% in **3** and **2**, respectively, what can be associated with a stronger binding of Li atoms with the [Cu₄(Hbes)₄] cores in **2** and **3**. This is also apparent from the considerable number of Li containing fragments, namely, [Cu₃(Hbes)₃Li]⁺ (m/z = 831), [Cu₂(Hbes)(H₂bes)₂Li]⁺ (m/z = 770), [Cu₂(Hbes)₂Li]⁺ (m/z = 555), and [Cu(H₂bes)₂Li]⁺ (m/z = 494), observed in the ESI-MS(+) spectra of **2** and/or **3**. In contrast, the spectrum of **1** shows slightly different [Cu₃(Hbes)₂(H₂bes)]⁺ (m/z = 825), [Cu₂(Hbes)(H₂bes)]⁺ (m/z = 550), and [Cu(H₂bes)(H₃bes)]⁺ (m/z = 489) peaks,

Table 1. Selected Distances (Å) and Angles (°) for 1, 2, and 3^a

compound	1	2	3
Cu1–N1	2.084(4)	2.085(4)	2.077(4)
Cu1–O1	1.924(3)	1.928(3)	1.923(3)
Cu1–O2	2.292(4)	2.303(4)	2.316(4)
Cu1–O7 ⁱ	1.904(3)	1.911(3)	1.918(3)
Cu1–O11	2.022(3)	2.020(3)	2.007(3)
Cu2–N2	2.026(4)	2.032(4)	2.025(4)
Cu2–O1	1.915(3)	1.922(3)	1.917(3)
Cu2–O6	2.290(4)	2.317(4)	2.307(5)
Cu2–O7	1.923(3)	1.928(3)	1.924(3)
Cu2–O8	2.010(3)	2.007(3)	2.016(4)
Li–O (H ₂ O)	1.927(10) avg.	1.995(12) avg.	1.992(12) avg.
Li–O3 (SO ₃)		2.039(19)	1.95(2)
Li–O10 (SO ₃)		1.880(18)	1.948(19)
Cu1...Cu1 ⁱ	3.058(1)	3.103(2)	3.111(1)
Cu1...Cu2	3.328(1)	3.316(2)	3.296(1)
Cu2...Cu2 ⁱ	5.930(1)	5.867(3)	5.830(2)
O1–Cu1–O7 ⁱ	153.18(14)	151.62(13)	151.20(15)
O1–Cu2–O7	88.38(13)	88.63(12)	88.62(14)
Cu1–O1–Cu2	120.24(16)	118.96(15)	118.28(16)
Cu1–O7–Cu2 ⁱ	122.55(16)	120.64(15)	120.23(17)

^aSymmetry transformation used to generate equivalent atoms: (i) $-x, y, 0.5 - z$.

corresponding to fragmentations with the stepwise loss of Cu atoms and Hbes moieties. The ESI-MS(–) plots further confirm the formulations of 1–3, revealing the characteristic [Cu₄(Hbes)₃(bes)][–] ($m/z = 1097$), [Cu₂(Hbes)(bes)][–] ($m/z = 549$), and [H₂bes][–] ($m/z = 212$) fragments with expected isotopic distribution patterns.

The IR spectra of 1–3 also show related features due to the presence of similar [Cu₄(μ-Hbes)₄(μ-carboxylate)][–] cores and aqua-lithium moieties. Hence, the characteristic bands in the 3600–3000 cm^{–1} range with maxima at 3389–3444 cm^{–1} are assigned to ν(OH) and ν(H₂O) vibrations, their broad character being associated with multiple hydrogen bonding interactions. In addition, the less intense bands at 1637–1638 cm^{–1} correspond to δ(OH) vibrations. Several bands due to ν_{as} and ν_s(CH) are also observed in the 2980–2865 cm^{–1} range. In all compounds, two sets of intense vibrations are detected in the 1590–1540 and 1455–1395 cm^{–1} ranges due to the asymmetric and symmetric modes of the carboxylate groups, respectively.^{11a,b} The spectra of all compounds also feature several strong bands with maxima in the 1232–1155 cm^{–1} interval due to ν(SO₃) vibrations. In addition, there is a number of bands (1100–900 cm^{–1}) that are associated to ν(C–X) (X = C, N, O) vibrations of the Hbes ligands. The UV–vis spectra of 1–3 are rather similar, exhibiting a broad absorption with maximum at 737–738 nm due to d–d transitions involving copper(II) ions, as well as an intense band with maximum at 294–307 nm due to π–π transitions of benzenecarboxylate ligands.^{11c}

The compounds 1–3 easily adsorb one additional water molecule from air as attested by elemental analyses. The differential thermal analyses of the resulting samples [Li(H₂O)₄][Cu₄(μ₂-Hbes)₄(μ₂-ba)]·2H₂O, [Cu₄(μ₃-Hbes)₄(μ₂-hba){Li(H₂O)₂}]_n·4nH₂O, and [Cu₄(μ₃-Hbes)₄(μ₂-dhba){Li(H₂O)₂}]_n·4nH₂O show multiple thermal effects over the 30–800 °C temperature range (Figure S6, Supporting Information). Hence, the material derived from 1 exhibits an endothermic process in the 80–140 °C range with the mass loss of 3.0% (calculated 2.7%) due to elimination of two

crystallization water molecules, whereas four coordinated H₂O ligands from [Li(H₂O)₄]⁺ cations are eliminated during the next exothermic effect in the 220–240 °C range, corresponding to the overall mass loss of 7.5% (calculated 8.1%). The materials derived from 2 and 3 also exhibit two-stage dehydration processes in the 40–150 and 220–235 °C intervals associated with removal of four crystallization (for 2, observed mass loss of 5.8%; calculated 5.3%) and two coordinated (observed overall mass loss of 9.3%; calculated 8.0%) water molecules, respectively. Further thermal effects above 240 °C are associated to the multistep decomposition of the ligands.

X-ray Crystal Structures. Compound 1 is a discrete 0D complex, the crystal structure of which bears the [Cu₄(μ₂-Hbes)₄(μ₂-ba)][–] anion, the [Li(H₂O)₄]⁺ cation, and one crystallization water molecule per formula unit (Figure 1). The tetracopper(II) cluster anion, having a crystallographic C₂ symmetry, consists of two pairs of the symmetry nonequivalent Cu1 and Cu2 atoms, two pairs of tri- and tetradentate bis-deprotonated μ₂-Hbes ligands, and one μ₂-benzoate ligand. The “central” five-coordinate Cu1 atoms adopt distorted {CuNO₄} square-pyramidal environments, filled by the μ-O1, μ-O7, and N1 atoms of μ₂-Hbes moieties [Cu1–O1 1.924(3), Cu1–O7ⁱ 1.904(3), Cu1–N1 2.084(4) Å], and the μ-O11 atom of benzoate ligand in basal positions [Cu1–O11 2.022(3) Å], while the remaining O2 atom (OH group) of μ₂-Hbes is located in the apical site [Cu1–O2 2.292(4) Å] (Table 1). The “side” Cu2 atoms are also five-coordinate and exhibit distorted {CuNO₄} square-pyramidal geometries which, in addition to the μ-O1, μ-O7, N2, and O6 atoms [Cu2–O1 1.915(3), Cu2–O7 1.923(3), Cu2–N2 2.026(4), Cu2–O6 2.290(4) Å], are filled with the O8 atom of the sulfonate group of μ₂-Hbes [Cu2–O8 2.010(3) Å]. The binding of adjacent μ₂-Hbes ligands is further reinforced by the intramolecular H-bonds between the OH groups (O2, O6) and the sulfonate O9 and O5 atoms (Figure 1). The four Cu atoms act as square pyramids fused via common vertexes into the [Cu₄(μ-O)₄(μ-COO)] cluster cores, wherein the metal centers are almost

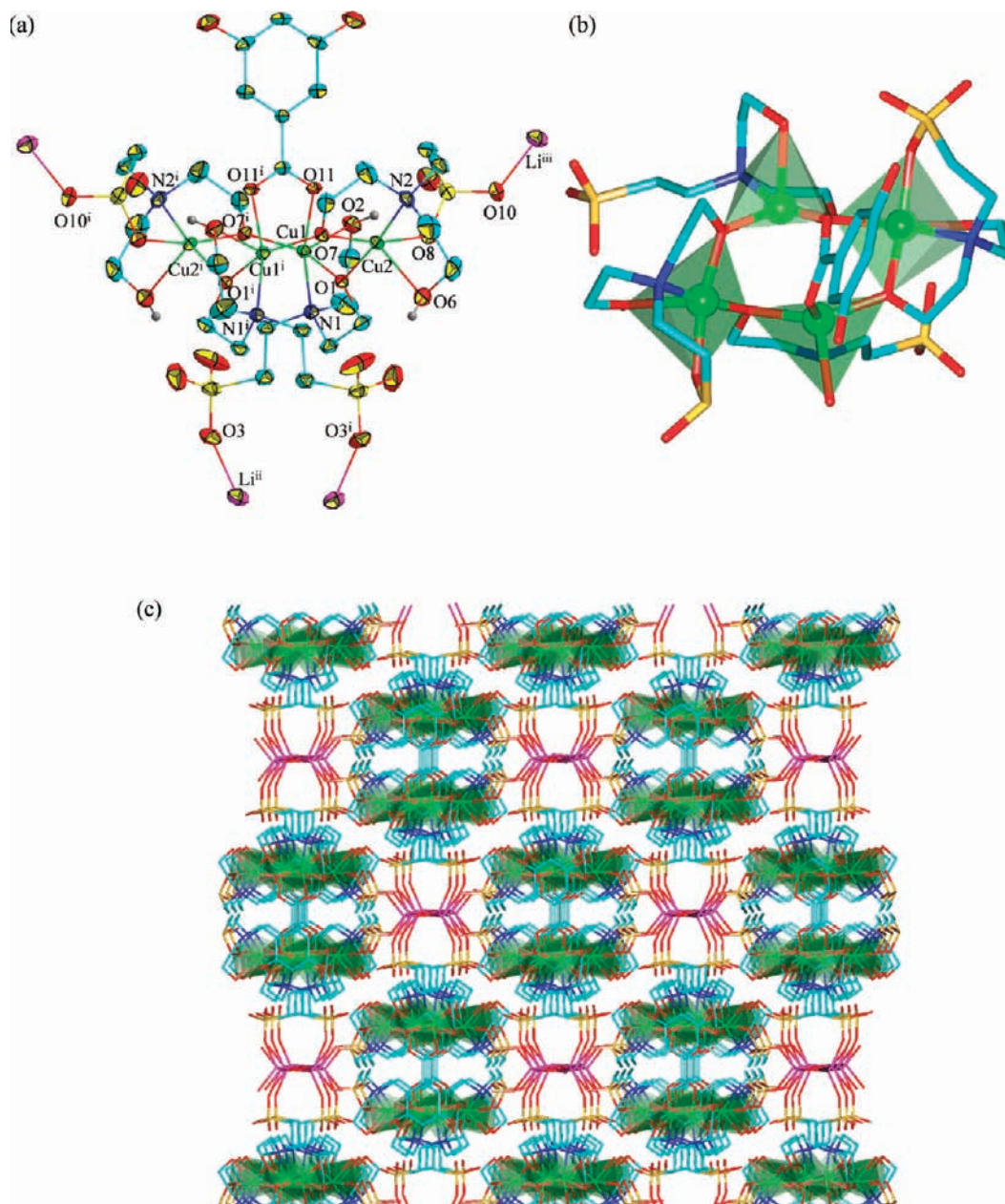


Figure 2. Structural fragments of **3**: (a) ellipsoid plot (30% probability) with the partial atom labeling scheme; (b) tetracopper(II) $[\text{Cu}_4(\mu_3\text{-Hbes})_4(\mu_2\text{-dhba})]^-$ unit with polyhedral representation of the coordination environments around Cu atoms; (c) infinite 3D noninterpenetrating metal–organic network (rotated view along the c axis). Further details: (a)–(c) H atoms, apart from those of OH groups in Hbes (a), crystallization water molecules, and aqua ligands within disordered $\text{Li}(\text{H}_2\text{O})_2$ moieties (a), are omitted for clarity. Color codes: Cu (green), Li (magenta), C (cyan), O (red), N (blue), S (yellow), H (gray). Symmetry codes are those of Table 1. Structural representations of **2** are quite similar to those of **3** (see Figure S2, Supporting Information).

coplanar, with the Cu...Cu separations ranging from 3.058(1) [Cu1...Cu1ⁱ] and 3.328(1) [Cu1...Cu2] to 5.930(1) Å [Cu2...Cu2ⁱ]. The quasi planarity of the Cu atoms is quite unusual for tetracopper(II) compounds.^{4,5b} The $[\text{Li}(\text{H}_2\text{O})_4]^+$ cation is composed of two pairs of symmetry nonequivalent water ligands and exhibits a distorted tetrahedral coordination environment. The anions and cations are in relatively close positions, and their linkage is realized through the strong O–H...O hydrogen bonds in which all the aqua ligands act as double H-bond donors to the sulfonate O atoms of Hbes. These multiple H-bonding interactions give rise to an infinite 3D supramolecular network (Figure S1, Supporting Information).

As in the case of **1**, the compounds **2** and **3** also crystallize in the monoclinic $C2/c$ space group, have comparable unit cell parameters, and bear similar tetracopper(II) $[\text{Cu}_4(\mu\text{-Hbes})_4(\mu\text{-carboxylate})]^-$ blocks (Figure 2a,b), which therefore are not discussed further in detail (bonding parameters are compared in Table 1). However, differently from **1**, the lithium atom in **2** and **3** is not bound to four water molecules but only to two, and the number of crystallization water molecules is also different. The $[\text{Li}(\text{H}_2\text{O})_2]^+$ groups, disordered and distributed in two positions, reach the tetrahedral coordination through two interactions with oxygen atoms of two sulfonate groups from $\mu_3\text{-Hbes}$ ligands (Figure 2a, b). The OH groups of hba and dhba in **2** and **3** are involved in intermolecular hydrogen

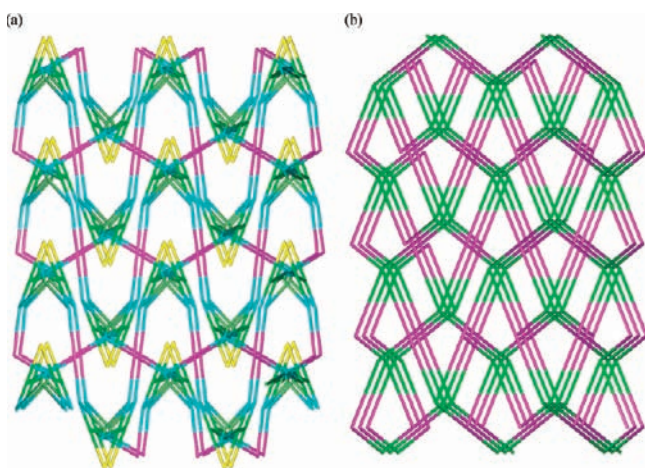
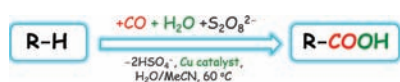


Figure 3. Topological representations (rotated views along the *a* axis) of the simplified underlying 3D networks in **2** and **3**: (a) topologically unique trinodal 3,3,4-connected net with the point symbol of $(4.6.8)_4(4^2.6)_2(6^2.16^2.18^2)$, composed of 4-connected Li nodes (magenta), 3-connected Cu1 nodes (green), centroids of 3-connected μ_3 -Hbes nodes (cyan), Cu2 linkers (pale green), and centroids of μ_2 -hba/ μ_2 -dhba linkers (yellow); (b) further simplified binodal 4,4-connected net with the *pts* topology, composed of 4-connected Li nodes (magenta) and centroids of 4-connected $[\text{Cu}_4(\mu_3\text{-Hbes})_4(\mu_2\text{-hba}/\mu_2\text{-dhba})]^-$ cluster nodes (green). For alternative topological representations, see Figures S4 and S5 in Supporting Information).

Scheme 2. Mild Single-Pot Hydrocarboxylation of C_n ($n = 2-9$) Alkanes into C_{n+1} Carboxylic Acids^a



^aR-H: ethane, propane, *n*-butane, *n*-pentane, *n*-hexane, *n*-heptane, *n*-octane, *n*-nonane, cyclopentane, cyclohexane, cycloheptane, and cyclooctane.

bonds with oxygen atoms of the sulfonate groups of different anions. In **2**, the OH group of hba is disordered and distributed in two positions, so that it forms the same hydrogen bonds of the two OH groups of dhba in **3**, explaining the very similar structural features of the two compounds. As a result, the $[\text{Cu}_4(\mu_3\text{-Hbes})_4(\mu_2\text{-hba}/\mu_2\text{-dhba})]^-$ blocks and disordered $[\text{Li}(\text{H}_2\text{O})_2]^+$ moieties in **2** and **3** are assembled into infinite 3D noninterpenetrating metal-organic networks (Figures 2c and S2 and S3, Supporting Information). It is noteworthy that, even if the anions in **2** and **3** are involved in intermolecular hydrogen bonds differently from **1**, their packing is comparable in all compounds and is not influenced by the different lithium units and the different number of water molecules.

Topological Analysis. To get a deeper insight into the intricate structures of coordination polymers **2** and **3**, we have performed their topological analysis by applying the concept of the simplified underlying net¹² and using TOPOS software package.¹³ Thus, by reducing μ_3 -Hbes and μ_2 -hba/ μ_2 -dhba ligands to their centroids and omitting H_2O molecules (disordered aqua-lithium moieties were treated as 4-connected nodes), the networks of **2** and **3** can be considered as underlying nets (Figure 3a) constructed from the 3-connected Cu1 and μ_3 -Hbes nodes and 4-connected Li nodes, as well as 2-connected Cu2 and μ_2 -hba/ μ_2 -dhba linkers. These trinodal 3,3,4-connected underlying nets in **2** and **3** are topologically equivalent, revealing a new type of topology that is defined by


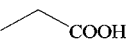
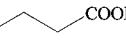
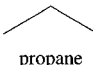
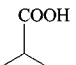
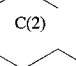
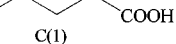
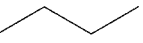
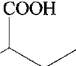
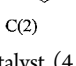
the point symbol of $(4.6.8)_4(4^2.6)_2(6^2.16^2.18^2)$, wherein the notations $(4.6.8)$, $(4^2.6)$, and $(6^2.16^2.18^2)$ correspond to the μ_3 -Hbes, Cu1, and Li nodes, respectively. To our knowledge,^{4,13,14} the present type of topology has not been reported previously. In contrast to many simple mono- and binodal CPs,^{1,2,12-14} the multinodal networks are still little represented, although the sweeping progress in crystal engineering is leading to an increasing number of such materials. In fact, a few 3,3,4-connected networks have emerged recently.¹⁵

To match the complex topology of the underlying nets in **2** and **3** with one of the frequent topological types encountered in CPs,¹²⁻¹⁴ we have performed their further simplification by treating the $[\text{Cu}_4(\mu_3\text{-Hbes})_4(\mu_2\text{-hba}/\mu_2\text{-dhba})]^-$ moieties as 4-connected cluster nodes (Cu_4). These, along with the 4-connected Li nodes, thus form a binodal 4,4-connected net with the *pts* (PtS, Cooperite) topology according to the RCSR¹⁴ classification, with the point symbol of $(4^2.8^4)$ and similar notations for both the Cu_4 and Li nodes (Figure 3b). Although a good number of CPs of the *pts* topological type are known,^{13,16} **2** and **3** represent the unique examples of the *pts* nets constructed from metal aminopolycarboxylate building blocks.

Mild Hydrocarboxylation of Alkanes into Carboxylic Acids. Although CPs are principally designed for use in heterogeneous catalysis,⁷ such compounds that possess some solubility in aqueous and/or organic medium can also be applied as precursors of catalytically active species in homogeneous catalytic reactions, particularly including those that mimic enzymatic processes. Hence, the aqueous solubility of **1-3** and their ability to dissociate into ionic species with labile and coordinatively unsaturated Cu centers can open up the use of these compounds as bioinspired catalyst precursors in homogeneous aqueous medium reactions. Following our general interest in the application of multicopper(II) complexes and coordination polymers in oxidation catalysis,^{5b-d,9,17} we have evaluated the activity of **1-3** for the mild hydrocarboxylation of C_n ($n = 2-9$) alkanes into C_{n+1} carboxylic acids. These transformations were run in stainless steel autoclaves by reacting, in $\text{H}_2\text{O}/\text{MeCN}$ medium at low temperature (60 °C), an alkane with carbon monoxide, water, and potassium peroxodisulfate, in the presence of **1**, **2**, or **3** (Scheme 2). As typical conditions, the previously optimized reaction parameters were applied.¹⁸ Different types of alkanes were used to show the substrate versatility of the present hydrocarboxylation protocol. Hence, the obtained results for the hydrocarboxylation of gaseous C_2 - C_4 , linear C_5 - C_9 , and cyclic C_5 - C_8 alkanes are summarized in Tables 2, 3, and 4, respectively. All the product yields along the discussion below are given in molar % based on alkanes.

Gaseous Alkanes. Compounds **1-3** catalyze the hydrocarboxylation of ethane to propanoic acid, propane to 2-methylpropanoic and butanoic acids, and *n*-butane to 2-methylbutanoic and pentanoic acids, whereas the attempted transformation of methane to acetic acid has so far been unsuccessful. Owing to the presence of only primary carbon atoms, C_2H_6 appears to be the least reactive alkane, providing the yields of propanoic acid in the 7-15% range (Table 2, entries 1-3). Although in the reactions with C_3H_8 and *n*- C_4H_{10} the yields of linear carboxylic acids (butanoic and pentanoic acids) also do not exceed 5-9%, the presence of significantly more reactive secondary carbon atoms in these alkanes allows their efficient transformation into the branched acids. In fact, the regioselectivity $\text{C}(1)/\text{C}(2)$ parameter (identical to the

Table 2. Cu-Catalyzed Single-Pot Hydrocarboxylation of Gaseous C_n ($n = 2-4$) Alkanes into the Corresponding C_{n+1} Carboxylic Acids^a

Entry	Alkane	Carboxylic acid product	Catalyst	Product yield, % ^b			Selectivity ^d C(1):C(2)
				C(1)	C(2)	Total ^c	
1			1	6.5	–	6.5	–
2	 ethane	 C(1)	2	15.2	–	15.2	–
3			3	8.1	–	8.1	–
4		 C(1)	1	6.3	56.2	62.5	1:27
5	 propane	 C(2)	2	8.1	66.5	74.6	1:25
6		 C(2)	3	8.6	69.0	77.6	1:24
7		 C(1)	1	1.2	26.6	27.8	1:33
8	 <i>n</i> -butane	 C(2)	2	4.4	61.0	65.4	1:21
9		 C(2)	3	5.2	58.3	63.5	1:17

^aReaction conditions: alkane (1.0 atm; 0.266 mmol), Cu catalyst (4.0 μ mol), $p(\text{CO}) = 10$ atm, $\text{K}_2\text{S}_2\text{O}_8$ (1.00 mmol), H_2O (2.0 mL)/MeCN (4.0 mL), 60 °C, 4 h in an autoclave (13.0 mL capacity). ^bMoles of product/100 mols of alkane. ^cYield of all products; the yields of ketones and alcohols are negligible (<1%) and thus are not indicated herein. Total TONs (moles of products/mol of catalyst) can be estimated as: $n(\text{alkane})/n(\text{catalyst}) \times \text{total \% yield} \times 10^{-2}$. ^dRegioselectivity parameters C(1)/C(2) that herein are identical to the primary/secondary carbon bond selectivity mean the normalized (for the relative number of H atoms) reactivities of hydrogen atoms at different positions of alkane chains.

primary/secondary carbon bond selectivity) values of 1:(24–27) and 1:(17–33) are observed in the reactions with propane and *n*-butane as substrates, respectively. The best yields of 2-methylpropanoic and 2-methylbutanoic acids attain 67–69 and 58–61% (entries 5, 6, 8, 9), respectively, when catalyst precursors **2** and **3** that show superior activity than that of **1** are used. The maximum total yields of carboxylic acid products in the hydrocarboxylations of propane and *n*-butane achieve values of 78 and 65%, correspondingly.

Liquid Linear Alkanes. The hydrocarboxylation reactions using linear C_5 – C_9 alkane substrates result in the single-pot formation of three or four isomeric monocarboxylic acid products (Table 3). The branched acids derived from the carboxylations at different secondary C(2), C(3), C(4), and C(5) carbon atoms within the hydrocarbon chain constitute the major products, while the corresponding linear (fatty) acids are only formed in minor amounts (<1.6% yield). Hence, isomeric carboxylic acids obtained from linear alkanes include (i) 2-methylpentanoic, 2-ethylbutanoic, and hexanoic acids from n - $C_5\text{H}_{12}$, (ii) 2-methylhexanoic, 2-ethylpentanoic, and heptanoic acids from n - $C_6\text{H}_{14}$, (iii) 2-methylheptanoic, 2-ethylhexanoic, 2-propylpentanoic, and octanoic acids from n - $C_7\text{H}_{16}$, (iv) 2-methyloctanoic, 2-ethylheptanoic, 2-propylhexanoic, and nonanoic acids from n - $C_8\text{H}_{18}$, and (v) 2-methylnonanoic, 2-ethyloctanoic, 2-propylheptanoic, 2-butylhexanoic, and decanoic acids from n - $C_9\text{H}_{20}$ (see Table 3 for structural formulas).


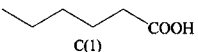
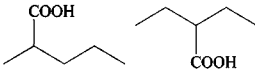
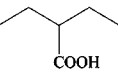
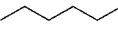
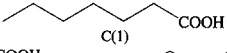
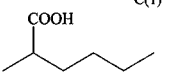
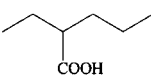
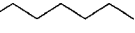
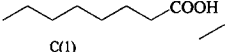
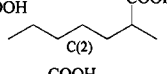
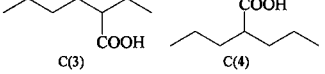

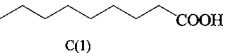
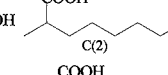
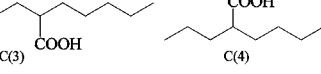
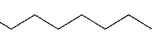
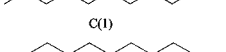
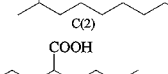
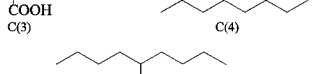
As in the case of gaseous alkanes, all the compounds **1**–**3** are active in the hydrocarboxylations of liquid alkanes and show somewhat comparable levels of activity (Table 3). However, **2** and/or **3** typically provide superior total yields in the hydrocarboxylations of n - $C_5\text{H}_{12}$ (37%, entry 3), n - $C_6\text{H}_{14}$ (32%, entry 5), and n - $C_7\text{H}_{16}$ (26%, entry 8), followed by the transformations of n - $C_9\text{H}_{20}$ (16%, entry 15) and n - $C_8\text{H}_{18}$ (11%,

entry 11) that are less reactive substrates. The highest turnover number (TON, moles of products/mol of catalyst precursor) attains 92 in the reaction with n - $C_5\text{H}_{12}$ (entry 3).

For the linear C_5 – C_9 alkanes, all the secondary carbon atoms are carboxylated without noticeable preference to any particular one, as attested by the C(1)/C(2)/C(3)/C(n) regioselectivities¹⁹ (normalized for the relative number of H atoms) of 1:25:24, 1:21:21, 1:21:22:18, 1:26:24:21, and 1:15:14:14:12 in the hydrocarboxylations, catalyzed by **3**, of n - $C_5\text{H}_{12}$, n - $C_6\text{H}_{14}$, n - $C_7\text{H}_{16}$, n - $C_8\text{H}_{18}$, and n - $C_9\text{H}_{20}$, respectively (Table 3). Hence, comparable yields of isomeric acid products are obtained in all systems. The regioselectivity parameters observed herein resemble those previously reported by us for the related hydrocarboxylations catalyzed by tri- and tetracopper(II) aminopolyalcoholate complexes,^{9a,18d} thus suggesting the involvement of the common sulfate radical $\text{SO}_4^{\bullet-}$ as an active species.^{18,20}

Liquid Cyclic Alkanes. In contrast to linear alkanes, the hydrocarboxylations of the cyclic C_5 – C_8 alkanes (Table 4) generate only one carboxylic acid product due to the presence of a single type of carbon atoms in these substrates. Thus, cyclopentanecarboxylic (30–42%, entries 1–3), cyclohexanecarboxylic (30–45%, entries 4–6), cycloheptanecarboxylic (24–29%, entries 7–9), and cyclooctanecarboxylic (2–8%, entries 10–12) acids are obtained with yields ranging from 2 to 45% upon hydrocarboxylations, catalyzed by **1**–**3**, of $C_5\text{H}_{10}$, $C_6\text{H}_{12}$, $C_7\text{H}_{14}$, and $C_8\text{H}_{18}$, respectively. Interestingly, compound **1** shows the highest activity in the reactions involving cyclohexane and cycloheptane (entries 4, 7), while the hydrocarboxylations of cyclopentane (entry 2) and cyclooctane (entry 12) are more efficient when catalyst precursors **2** and **3** are used, respectively. The maximum overall TON of 118 is obtained in the hydrocarboxylation of cyclopentane catalyzed

Table 3. Cu-Catalyzed Single-Pot Hydrocarboxylation of Linear C_n (n = 5–9) Alkanes into the Corresponding C_{n+1} Carboxylic Acids^a

Entry	Alkane	Carboxylic acid product	Catalyst	Product yield, % ^b					Regioselectivity ^d C(1):C(2):C(3):C(n)
				C(1)	C(2)	C(3)	C(4)	Total ^c	
1	 n-pentane	 C(1)	1	1.6	20.2	9.2	–	31.0	1:19:18
2		 C(2)	2	1.4	23.0	10.0	–	34.4	1:25:24
3		 C(3)	3	1.4	23.7	11.6	–	36.7	1:25:24
4	 n-hexane	 C(1)	1	0.6	7.4	7.9	–	15.9	1:19:20
5		 C(2)	2	1.2	15.6	15.3	–	32.1	1:20:19
6		 C(3)	3	1.0	13.8	13.9	–	28.7	1:21:21
7	 n-heptane	 C(1)	1	0.9	9.2	10.1	4.5	24.7	1:15:17:15
8		 C(2)	2	0.8	10.6	10.3	4.4	26.1	1:14:14:12
9		 C(3)	3	0.6	8.5	8.9	3.7	21.7	1:21:22:18
10	 n-octane	 C(1)	1	0.2	2.2	2.0	1.8	6.2	1:19:18:16
11		 C(2)	2	0.2	3.7	3.7	3.4	11.0	1:23:23:21
12		 C(3)	3	0.15	2.6	2.2	2.0	7.0	1:26:24:21
13	 n-nonane	 C(1)	1	0.3	4.0	4.0	4.0 (1.4) ^e	13.7	1:20:20:20:14
14		 C(2)	2	0.3	4.4	4.2	4.2 (1.9) ^e	15.0	1:22:21:21:19
15		 C(3)	3	0.5	4.9	4.7	4.7 (1.6) ^e	16.4	1:15:14:14:12

^aReaction conditions: alkane (1.00 mmol), Cu catalyst (4.0 μmol), *p*(CO) = 20 atm, K₂S₂O₈ (1.50 mmol), H₂O (2.0 mL)/MeCN (4.0 mL), 60 °C, 4 h in an autoclave (13.0 mL capacity). ^bMoles of product/100 mols of alkane. ^cYield of all products; the yields of ketones and alcohols are negligible (<1%) and thus are not indicated herein. Total TONs (moles of products/mol of catalyst) can be estimated as: *n*(alkane)/*n*(catalyst) × total % yield × 10⁻². ^dRegioselectivity parameters C(1)/C(2)/C(3)/C(*n*) mean the normalized (for the relative number of H atoms) reactivities of hydrogen atoms at different positions of linear alkane chains. ^eYield of the C(5) product is given in brackets.

by 2 (Table 4, entry 2). A particular characteristic of the transformations involving cycloalkanes as substrates consists of the formation of the oxidation products (cyclic ketones and alcohols) in up to 13% overall yields (Table 4). On the contrary, the yields of ketones and alcohols are negligible (typically below 1%) in the reactions of gaseous and liquid linear alkanes.

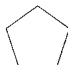
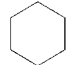
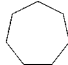
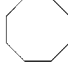
Proposed Mechanism. A simplified free-radical mechanism (Scheme 3) can be proposed for the hydrocarboxylations of C₂–C₉ alkanes on the basis of extensive background accumulated for alkane carboxylation reactions in either H₂O/MeCN¹⁸ or CF₃COOH²¹ medium. Further evidence for a free-radical mechanism is provided by the type of regioselectivity parameters along with the detected suppression of the formation of carboxylic acids in the experiments undertaken in the presence of a carbon-centered radical trap (CBrCl₃). The mechanism bears the following steps: (1) the generation of the alkyl radicals R• from an alkane [formed via H abstraction by

sulfate radical SO₄^{•-} derived from K₂S₂O₈], (2) the carbon-ylation of R• by CO to furnish the acyl radicals RCO•, (3) the oxidation of RCO• by CO to copper(II) species to the acyl cations RCO⁺ [via the Cu^{II}/Cu^I redox couple], (3') the regeneration of the Cu^{II} form upon oxidation of Cu^I by K₂S₂O₈, and (4) the hydrolysis of RCO⁺ to yield the carboxylic acid products.^{5b,18} The last step was previously confirmed by us on the basis of experiments with ¹⁸O-labeled H₂O and theoretical calculations.^{18a}

CONCLUSIONS

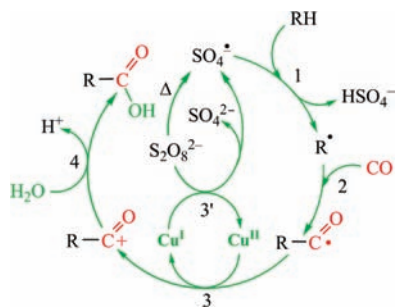
In the present work, we have shown that the common biobuffer H₃bes provides a convenient hydrosoluble *N,O*-building block for the generation, by aqueous medium self-assembly, of new heterometallic Cu^{II}/Li metal–organic materials 1–3 that bear a rare type of tetracopper(II) cores. A key role in defining the dimensionality of the obtained compounds is played by the type of ancillary benzenecarboxylate ligand, a slight modifica-

Table 4. Cu-Catalyzed Single-Pot Hydrocarboxylation of C_n ($n = 5-8$) Cycloalkanes into the Corresponding C_{n+1} Cycloalkancarboxylic Acids^a

Entry	Cycloalkane	Catalyst	Product yield, % ^b			
			Carboxylic acid	Ketone	Alcohol	Total ^c
1		1	29.5	2.7	0.4	32.6
2		2	42.0	4.4	0.8	47.2
3		3	30.9	3.7	0.5	35.1
4 ^d		1	44.8	1.7	0.5	47.1
5 ^d		2	43.8	1.7	0.5	46.0
6 ^d		3	30.3	1.4	0.5	32.1
7		1	28.5	7.8	1.8	38.1
8		2	24.6	7.2	1.6	33.4
9		3	23.7	6.0	1.4	31.1
10		1	2.0	2.7	2.0	6.2
11		2	6.5	8.8	3.5	18.8
12		3	7.8	7.7	2.9	18.4

^aCyclic ketones and alcohols are also formed as products of cycloalkane oxidations. Reaction conditions (unless stated otherwise): cycloalkane (1.00 mmol), Cu catalyst (4.0 μ mol), $p(\text{CO}) = 20$ atm, $\text{K}_2\text{S}_2\text{O}_8$ (1.50 mmol), H_2O (2.0 mL)/MeCN (4.0 mL), 60 °C, 4 h in an autoclave (13.0 mL capacity). ^bMoles of product/100 mols of alkane. ^cYield of all products. Total TONs (moles of products/mol of catalyst) can be estimated as: $n(\text{alkane})/n(\text{catalyst}) \times \text{total \% yield} \times 10^{-2}$. ^d H_2O (3.0 mL)/MeCN (3.0 mL), 50 °C.

Scheme 3. Proposed Mechanism for the Copper-Catalyzed Hydrocarboxylation of Alkanes (RH) to Carboxylic Acids (RCOOH)



tion of which via the introduction of one or two OH groups resulted in the heterometallic CPs 2 and 3. Their crystal structures feature infinite 3D noninterpenetrating networks that can be described as the trinodal 3,3,4-connected underlying nets with an unprecedented topology defined by the point symbol of $(4.6.8)_4(4^2.6)_2(6^2.16^2.18^2)$ or, after further simplification, as the binodal 4,4-connected nets with the pts (PtS) topology. The study thus also contributes to the identification and classification of CPs with new topologies.¹²

Besides, compounds 2 and 3 represent rare examples of CPs that show solubility in water, thus opening up their application in aqueous-phase catalysis. In fact, we have found that both the discrete complex 1 and the polymers 2 and 3 can act as versatile and efficient homogeneous catalyst precursors for the mild single-pot hydrocarboxylation, by CO and H_2O , of various gaseous, linear, and cyclic C_n ($n = 2-9$) alkanes into the

corresponding C_{n+1} carboxylic acids. Their total yields obtained in the present work are very high (up to 78% based on alkane), considering the exceptional inertness of saturated hydrocarbons and the fact that the present reactions involve C–H bond cleavage, C–C bond formation, and proceed in an acid-solvent-free $\text{H}_2\text{O}/\text{MeCN}$ medium (water plays a main role as a reagent, besides being a mere solvent component) and at a very mild temperature (60 °C). Furthermore, these hydrocarboxylations contrast with most of the state-of-the-art processes for the relatively mild transformations of alkanes that require the use of strongly acidic reaction media (concentrated trifluoroacetic or sulfuric acid or a superacid).^{22,23}

In summary, the study provides a contribution to the sweeping research on coordination polymers,^{1-3,7,8} namely, concerning (i) the development of aqueous medium self-assembly synthetic protocols, (ii) the underexplored application of biobuffers as versatile building blocks for the design of CPs, (iii) the identification of new topological types, (iv) the synthesis of rare hydrosoluble metal–organic materials, and (v) the use of CPs in oxidation catalysis. The exploration of these and other research directions will be pursued in our future studies, aiming at the design of new functional metal–organic networks toward their application in catalysis.

EXPERIMENTAL SECTION

Materials and Methods. All synthetic work was performed in air and at room temperature (rt, ~ 25 °C). All chemicals were obtained from commercial sources and used as received. C, H, N, and S elemental analyses were carried out by the Microanalytical Service of the Instituto Superior Técnico. Infrared spectra ($4000-400$ cm^{-1}) were recorded on a BIO-RAD FTS 3000MX instrument in KBr pellets (abbreviations: vs, very strong; s, strong; m, medium; w, weak; br, broad; sh, shoulder). The UV–vis spectra were recorded at rt on a Jasco model 7800 UV–vis spectrophotometer, using ca. 10^{-3} M solutions of 1–3 in water. ESI-MS(\pm) spectra were run on a 500-MS LC Ion Trap instrument (Varian Inc., Alto Palo, CA, USA) equipped with an electrospray (ESI) ion source, using ca. 10^{-3} M solutions of 1–3 in water. Differential thermal analyses were performed with a Perkin-Elmer STA 6000 instrument. The crystalline samples (5–12 mg) were heated in air at the rate of 10 °C/min in the 30–800 °C temperature range. Gas chromatography (GC) analyses were performed on a Fisons Instruments GC 8000 series gas chromatograph with a DB WAX (J&W) capillary column (30 m \times 0.25 mm \times 0.25 μm ; helium carrier gas) and using Jasco-Borwin v.1.50 software.

General synthetic procedure for 1–3. To an aqueous solution (5.0 mL) of $\text{Cu}(\text{NO}_3)_2 \cdot 2.5\text{H}_2\text{O}$ (116 mg, 0.50 mmol) was added N,N -bis(2-hydroxyethyl)-2-aminoethanesulfonic acid [H_3bes] (107 mg, 0.5 mmol) with continuous stirring at rt. Benzoic acid (Hba; 61 mg, 0.50 mmol) for 1, 3-hydroxybenzoic acid (Hhba; 69 mg, 0.50 mmol) for 2, or 3,5-dihydroxybenzoic acid (Hdhba; 77 mg, 0.50 mmol) for 3 was dissolved in an aqueous 1 M solution of LiOH (1.5 mL, 1.50 mmol) and added to the reaction mixture. The resulting cloudy solution was stirred for 1 day and then filtered off. The filtrate was left to evaporate in a beaker at rt. Greenish blue (turquoise) crystals, including those of X-ray quality, were formed in 1–2 weeks, then collected, and dried in air to give compounds 1–3 in ca. 70% yield, based on copper(II) nitrate.

[Li(H₂O)₄][Cu₄(μ_2 -Hbes)₄(μ_2 -ba)] \cdot H₂O (1). Anal. Calcd for 1 + H₂O: C₃₁H₆₉Cu₄LiN₄O₂₈S₄ (MW 1335.3): C 27.88, H 5.21, N 4.20, S 9.61; found: C 27.81, H 4.94, N 4.16, S 9.22. Solubility in H₂O: $S_{25}^\circ \text{C} \approx 6$ mg mL⁻¹. IR (KBr): 3399 vs br. $\nu(\text{H}_2\text{O}) + \nu(\text{OH})$, 2980 w and 2942 m $\nu_{\text{as}}(\text{CH})$, 2874 m $\nu_{\text{s}}(\text{CH})$, 1655 m br. $\delta(\text{OH})$, 1472 w, 1361 w, 1332 w, 1235 sh. and 1209 s, 1185 s and 1153 vs $\nu(\text{SO}_3)$, 1076 s, 1049 s, 1025 vs, 983 w, 905 s, 814 w, 736 s br., 680 s, 570 m, 525 w and 468 w cm^{-1} . UV–vis (H₂O): λ_{max} nm (ϵ , L mol⁻¹ cm⁻¹): 737 (450) and 294 (2475). ESI-MS(\pm) (H₂O), selected fragments with relative abundance >10%, MS(+): m/z : 1105 (40%) [$\text{Cu}_4(\text{Hbes})_4\text{Li}$]⁺,

Table 5. Crystal Data and Structure Refinement Details for Compounds 1–3

compound	1	2	3
formula	C ₃₁ H ₆₇ Cu ₄ LiN ₄ O ₂₇ S ₄	C ₃₁ H ₆₇ Cu ₄ LiN ₄ O ₂₈ S ₄	C ₃₁ H ₆₇ Cu ₄ LiN ₄ O ₂₉ S ₄
fw	1317.23	1333.23	1349.23
T (K)	203(2)	273(2)	273(2)
λ (Å)	0.71073	0.71073	0.71073
crystal system	monoclinic	monoclinic	monoclinic
space group	C2/c	C2/c	C2/c
a (Å)	18.165(3)	19.013(10)	19.137(5)
b (Å)	20.857(4)	20.508(9)	20.483(5)
c (Å)	14.123(3)	14.336(6)	14.562(3)
β (deg)	113.741(2)	116.428(8)	117.006(4)
V (Å ³)	4898.0(16)	5006(4)	5085(2)
Z	4	4	4
ρ _{calcd} (g/cm ³)	1.786	1.769	1.762
μ(Mo Kα) (mm ⁻¹)	1.977	1.939	1.909
no. of collected reflns	28584	25924	20877
no. of unique reflns	5619	4671	3689
final R1 ^a , wR2 ^b (I ≥ 2σ)	0.0569, 0.0977	0.0402, 0.1057	0.0382, 0.0814

$$^a R1 = \sum ||F_o| - |F_c|| / \sum |F_o| \quad ^b wR2 = [\sum [w(F_o^2 - F_c^2)^2] / \sum [w(F_o^2)^2]]^{1/2}$$

825 (30%) [Cu₃(Hbes)₂(H₂bes)]⁺, 770 (50%) [Cu₂(Hbes)(H₂bes)₂Li]⁺, 550 (25%) [Cu₂(Hbes)(H₂bes)]⁺, 489 (20%) [Cu(H₂bes)(H₃bes)]⁺, 275 (100%) [Cu(H₂bes)]⁺. MS(-): m/z: 1097 (10%) [Cu₄(Hbes)₃(bes)]⁻, 761 (10%) [Cu₂(Hbes)₂(bes)]⁻, 549 (20%) [Cu₂(Hbes)(bes)]⁻, 212 (100%) [H₂bes]⁻.

[Cu₄(μ₃-Hbes)₄(μ₂-hba)(Li(H₂O)₂)_n·3nH₂O (2). Anal. Calcd for 2 + H₂O: C₃₁H₆₉Cu₄LiN₄O₂₉S₄ (MW 1351.3): C 27.55, H 5.15, N 4.15, S 9.49; found: C 27.42, H 4.80, N 4.13, S 9.30. Solubility in H₂O: S_{25 °C} ≈ 5 mg mL⁻¹. IR (KBr): 3389 vs br. ν(H₂O)+ν(OH), 2942 w and 2920 w ν_{as}(CH), 2876 m ν_s(CH), 1638 m br. δ(OH), 1591 w, 1546 vs ν_{as}(COO), 1451 w and 1401 s ν_s(COO), 1471 w, 1360 w, 1331 w, 1299 w, 1232 vs and 1187 and 1155 s ν(SO₃), 1071 s, 1050 s, 1024 s, 983 w, 963 w, 905 s, 882 w, 825 w, 802 m, 783 m, 751 s, 676 s, 558 m, 522 w, 502 w, 464 w and 427 w cm⁻¹. UV-vis (H₂O): λ_{max} nm (ε, L mol⁻¹ cm⁻¹): 738 (555) and 304 (2610). ESI-MS(±) (H₂O), selected fragments with relative abundance >10%, MS(+): m/z: 1105 (100%) [Cu₄(Hbes)₄Li]⁺, 885 (55%) [Cu₄(Hbes)₂(bes)]⁺, 831 (35%) [Cu₃(Hbes)₃Li]⁺, 770 (50%) [Cu₂(Hbes)(H₂bes)₂Li]⁺, 555 (35%) [Cu₂(Hbes)₂Li]⁺, 494 (15%) [Cu(H₂bes)₂Li]⁺, 275 (30%) [Cu(H₂bes)]⁺. MS(-): m/z: 1097 (25%) [Cu₄(Hbes)₃(bes)]⁻, 823 (15%) [Cu₃(Hbes)₂(bes)]⁻, 549 (30%) [Cu₂(Hbes)(bes)]⁻, 212 (100%) [H₂bes]⁻.

[Cu₄(μ₃-Hbes)₄(μ₂-dhba)(Li(H₂O)₂)_n·3nH₂O (3). Anal. Calcd for 3 + H₂O: C₃₁H₆₉Cu₄LiN₄O₃₀S₄ (MW 1367.3): C 27.23, H 5.09, N 4.10, S 9.38; found: C 27.04, H 4.79, N 4.05, S 9.25. Solubility in H₂O: S_{25 °C} ≈ 5 mg mL⁻¹. IR (KBr): 3444 vs br. ν(H₂O)+ν(OH), 2941 m and 2920 w ν_{as}(CH), 2887 w and 2866 w ν_s(CH), 1637 m br. δ(OH), 1601 w, 1546 vs ν_{as}(COO), 1453 w and 1396 s ν_s(COO), 1364 w, 1332 w, 1287 w, 1218 vs and 1190 and 1158 s ν(SO₃), 1070 s, 1049 s, 1024 s, 985 m, 963 w, 906 s, 882 w, 851 w, 799 w, 752 s, 663 s, 557 w, 524 w, 501 w and 425 w cm⁻¹. UV-vis (H₂O): λ_{max} nm (ε, L mol⁻¹ cm⁻¹): 738 (545) and 307 (2555). ESI-MS(±) (H₂O), selected fragments with relative abundance >10%, MS(+): m/z: 1105 (70%) [Cu₄(Hbes)₄Li]⁺, 885 (50%) [Cu₄(Hbes)₂(bes)]⁺, 831 (40%) [Cu₃(Hbes)₃Li]⁺, 770 (70%) [Cu₂(Hbes)(H₂bes)₂Li]⁺, 550 (30%) [Cu₂(Hbes)₂Li]⁺, 494 (35%) [Cu(H₂bes)₂Li]⁺, 275 (100%) [Cu(H₂bes)]⁺. MS(-): m/z: 1097 (20%) [Cu₄(Hbes)₃(bes)]⁻, 823 (15%) [Cu₃(Hbes)₂(bes)]⁻, 761 (20%) [Cu₂(Hbes)₂(bes)]⁻, 549 (25%) [Cu₂(Hbes)(bes)]⁻, 212 (100%) [H₂bes]⁻.

X-ray Crystal Structure Determinations. The intensity data of compounds 1–3 were collected on a Bruker SMART 1000 single crystal diffractometer using a graphite monochromated Mo Kα radiation. The structures were solved by Fourier methods and refined by full-matrix least-squares procedures, first with isotropic thermal parameters and then with anisotropic thermal parameters in the last few cycles of refinement for all the nonhydrogen atoms.²⁴ In 2 and 3,

the [Li(H₂O)₂]⁺ moiety is disordered and distributed in two positions completing the tetrahedral coordination with two oxygen atoms of two SO₃ groups of different anions. As already pointed out, the OH group of hba in 2 is disordered and distributed in two positions, so that it forms the same hydrogen bonds of the two OH groups of dhba in 3, explaining the comparable packing patterns and unit cells of the two compounds. The hydrogen atoms of the anions were introduced into the geometrically calculated positions and refined riding on the corresponding parent atoms. In 1, the hydrogen atoms of the water molecules bonded to the Li atom were found and refined isotropically. Crystal data and details of data collection for 1–3 are summarized in Table 5.

Hydrocarboxylation of Alkanes. In a typical experiment, the reaction mixtures were prepared as follows: to 4.0 μmol of the compounds 1, 2, or 3 contained in a 13.0 mL stainless steel autoclave, equipped with a Teflon-coated magnetic stirring bar, were added 1.00–1.50 mmol of K₂S₂O₈, 2.0 mL of H₂O, 4.0 mL of MeCN (total solvent volume was 6.0 mL), and 1.00 mmol of alkane (if liquid). Then, the autoclave was closed and flushed with CO three times to remove the air and finally pressurized with 1.0 atm of alkane (if gaseous) and 10–20 atm of CO. The reaction mixture was typically stirred for 4 h at 60 °C using a magnetic stirrer and an oil bath, where upon it was cooled in an ice bath, degassed, opened, and transferred to a flask. Diethyl ether (9.0 mL) and 90 μL of cycloheptanone (typical GC internal standard) were added. In the case of cycloheptane hydrocarboxylation, cyclohexanone (90 μL) was used as a GC standard. The obtained mixture was vigorously stirred for 10 min, and the organic layer was analyzed by gas chromatography (internal standard method), revealing the formation of the corresponding monocarboxylic acids as the dominant products.

In the reactions with cycloalkane substrates, cyclic ketones and alcohols were also formed as byproducts of partial alkane oxidation, whereas in the transformations of linear alkanes the generation of the corresponding oxygenates was negligible (their overall yields were not exceeding 1.0%). Some reaction mixtures of cycloalkane hydrocarboxylations were also subjected to GC analyses before and after the treatment with PPh₃ (classical method for the determination of alkyl hydroperoxides),^{23a} revealing that no variation in alcohol and ketone yields upon addition of PPh₃ was detected. This suggests that alkyl hydroperoxides either do not form or, if formed, fully decompose into the corresponding cyclic alcohols and ketones along the reaction.

Blank tests indicated that the hydrocarboxylations also proceeded in the metal-free systems, although typically leading to 2–5 times inferior yields of carboxylic acids in comparison with the Cu-catalyzed transformations.¹⁸ The alkane hydrocarboxylations do not undergo either in sole H₂O or MeCN solvent. The formation of dicarboxylic

acids was also not observed. Apart from $K_2S_2O_8$, the use of other oxidants (H_2O_2 , O_2 , $t\text{-BuOOH}$, or KIO_4) in the present hydrocarboxylations has so far been unsuccessful.^{18b}

■ ASSOCIATED CONTENT

■ Supporting Information

Additional structural representations (Figures S1–S5), differential thermal analysis plots (Figure S6), and crystallographic file in CIF format for 1–3. This material is available free of charge via the Internet at <http://pubs.acs.org>.

■ AUTHOR INFORMATION

Corresponding Author

*E-mail: kirillov@ist.utl.pt (A.M.K.); pombeiro@ist.utl.pt (A.J.L.P.). Phone: +351 218419207/37. Fax: +351 218464455.

Notes

The authors declare no competing financial interest.

■ ACKNOWLEDGMENTS

This work was supported by the Foundation for Science and Technology (FCT) (projects PTDC/QUI-QUI/102150/2008, PTDC/QUI-QUI/121526/2010, and PEst-OE/QUI/UI0100/2011), Portugal, as well as its “Science 2007” program. We thank Dr. M. C. Oliveira for ESI-MS measurements (IST-node of the RNEM/FCT).

■ REFERENCES

(1) For state-of-the-art books on the topic, see: (a) Farrusseng, D., Ed. *Metal-Organic Frameworks: Applications from Catalysis to Gas Storage*; Wiley: Weinheim, 2011. (b) Schroder, M., Ed. *Functional Metal-Organic Frameworks: Gas Storage, Separation and Catalysis*; Springer: New York, 2010. (c) MacGillivray, L. R., Ed. *Metal-Organic Frameworks: Design and Application*; Wiley-Interscience: New York, 2010. (d) Batten, S. R., Turner, D. R., Neville, S. M. *Coordination Polymers: Design, Analysis and Application*; Royal Society of Chemistry: London, 2009. (e) Hong, M.-C., Chen, L., Ed. *Design and Construction of Coordination Polymers*; Wiley: New York, 2009.

(2) For selected reviews, see: (a) Fromm, K. M.; Sagué, J. L.; Mirolo, L. *Macromol. Symp.* **2010**, 291–292, 75. (b) Janiak, C.; Vieth, J. K. *New J. Chem.* **2010**, 34, 2366. (c) Kirillov, A. M. *Coord. Chem. Rev.* **2011**, 255, 1603. (d) Perry, J. J., IV; Perman, J. A.; Zaworotko, M. J. *Chem. Soc. Rev.* **2009**, 38, 1400. (e) Tranchemontagne, D. J.; Mendozacortes, J. L.; O’Keeffe, M.; Yaghi, O. M. *Chem. Soc. Rev.* **2009**, 38, 1257. (f) Qiu, S.; Zhu, G. *Coord. Chem. Rev.* **2009**, 253, 2891. (g) Robin, A. Y.; Fromm, K. M. *Coord. Chem. Rev.* **2006**, 250, 2127. (h) Kitagawa, S.; Uemura, K. *Chem. Soc. Rev.* **2005**, 34, 109. (i) Rao, C. N. R.; Natarajan, S.; Vaidhyanathan, R. *Angew. Chem., Int. Ed.* **2004**, 43, 1466. (j) Kitagawa, S.; Kitaura, R.; Noro, S. *Angew. Chem., Int. Ed.* **2004**, 43, 2334. (k) Janiak, C. *Dalton Trans.* **2003**, 2781. (l) James, S. L. *Chem. Soc. Rev.* **2003**, 32, 276. (m) Moulton, B.; Zaworotko, M. J. *Chem. Rev.* **2001**, 101, 1629.

(3) Champness, N. R. *Dalton Trans.* **2011**, 40, 10311.

(4) See the Cambridge Structural Database (CSD, version 5.32, Nov. 2011): Allen, F. H. *Acta Crystallogr.* **2002**, B58, 380.

(5) (a) Kirillov, A. M.; Wieczorek, S. W.; Lis, A.; Guedes da Silva, M. F. C.; Florek, M.; Król, J.; Staroniewicz, Z.; Smolenski, P.; Pombeiro, A. J. L. *Cryst. Growth Des.* **2011**, 11, 2711. (b) Kirillov, A. M.; Coelho, J. A. S.; Kirillova, M. V.; Guedes da Silva, M. F. C.; Nesterov, D. S.; Gruenwald, K. R.; Haukka, M.; Pombeiro, A. J. L. *Inorg. Chem.* **2010**, 49, 6390. (c) Kirillova, M. V.; Kirillov, A. M.; Guedes da Silva, M. F. C.; Pombeiro, A. J. L. *Eur. J. Inorg. Chem.* **2008**, 3423. (d) Karabach, Y. Y.; Kirillov, A. M.; Guedes da Silva, M. F. C.; Kopylovich, M. N.; Pombeiro, A. J. L. *Cryst. Growth Des.* **2006**, 6, 2200.

(6) (a) Gasnier, A.; Barbe, J.-M.; Bucher, C.; Duboc, C.; Moutet, J.-C.; Saint-Aman, E.; Terech, P.; Royal, G. *Inorg. Chem.* **2010**, 49, 2592. (b) Folch, B.; Larionova, J.; Guari, Y.; Molvinger, K.; Luna, C.;

Sangregorio, C.; Innocenti, C.; Caneschi, A.; Guerin, C. *Phys. Chem. Chem. Phys.* **2010**, 12, 12760. (c) Friese, V. A.; Kurth, D. G. *Coord. Chem. Rev.* **2008**, 252, 199. (d) Guari, Y.; Larionova, J.; Molvinger, K.; Folch, B.; Guerin, C. *Chem. Commun.* **2006**, 2613. (e) Vermond, T.; van Steenberg, M. J.; Besseling, N. A. M.; Marcelis, A. T. M.; Hennink, W. E.; Sudholter, E. J. R.; Stuart, M. A. C. *J. Am. Chem. Soc.* **2004**, 126, 15802.

(7) For recent reviews on the use of CPs in catalysis, see: (a) Ma, L.-Q.; Abney, C.; Lin, W.-B. *Chem. Soc. Rev.* **2009**, 38, 1248. (b) Lee, J.-Y.; Farha, O. K.; Roberts, J.; Scheidt, K. A.; Nguyen, S. T.; Hupp, J. T. *Chem. Soc. Rev.* **2009**, 38, 1450. (c) Farrusseng, D.; Aguado, S.; Pinel, C. *Angew. Chem., Int. Ed.* **2009**, 48, 7502. (d) Corma, A.; Garcia, H.; Xamena, F. X. L. *Chem. Rev.* **2010**, 110, 4606. (e) Ranocchiaro, M.; van Bokhoven, J. A. *Phys. Chem. Chem. Phys.* **2011**, 13, 6388.

(8) For recent reviews on bioactive metal–organic frameworks, see: (a) McKinlay, A. C.; Morris, R. E.; Horcajada, P.; Férey, G.; Gref, R.; Couvreur, P.; Serre, C. *Angew. Chem., Int. Ed.* **2010**, 49, 6260. (b) Horcajada, P.; Gref, R.; Baati, T.; Allan, P. K.; Maurin, G.; Couvreur, P.; Férey, G.; Morris, R. E.; Serre, C. *Chem. Rev.* **2012**, 112, 1232.

(9) (a) Kirillov, A. M.; Karabach, Y. Y.; Kirillova, M. V.; Haukka, M.; Pombeiro, A. J. L. *Dalton Trans.* **2011**, 40, 6378. (b) Karabach, Y. Y.; Guedes da Silva, M. F. C.; Kopylovich, M. N.; Gil-Hernández, B.; Sanchiz, J.; Kirillov, A. M.; Pombeiro, A. J. L. *Inorg. Chem.* **2010**, 49, 11096. (c) Kirillov, A. M.; Kopylovich, M. N.; Kirillova, M. V.; Haukka, M.; da Silva, M. F. C. G.; Pombeiro, A. J. L. *Angew. Chem., Int. Ed.* **2005**, 44, 4345.

(10) (a) Lieberman, R. L.; Rosenzweig, A. C. *Nature* **2005**, 434, 177. (b) Chan, S. I.; Wang, V. C.-C.; Lai, J. C.-H.; Yu, S. S.-F.; Chen, P. P.-Y.; Chen, K. H.-C.; Chen, C.-L.; Chan, M. K. *Angew. Chem., Int. Ed.* **2007**, 46, 1992.

(11) (a) Nakamoto, K. *Infrared and Raman Spectra of Inorganic and Coordination Compounds*, 5th ed.; Wiley: New York, 1997. (b) SDBSWeb: <http://riodb01.ibase.aist.go.jp/sdbs/> (National Institute of Advanced Industrial Science and Technology, 2012). (Accessed January 2012). (c) Lever, A. B. P. *Inorganic Electronic Spectroscopy*, 2nd ed.; Elsevier: Amsterdam, 1984.

(12) (a) Blatov, V. A.; Proserpio, D. M. In *Modern Methods of Crystal Structure Prediction*; Oganov, A. R., Ed.; Wiley: Weinheim, 2010; pp 1–28. (b) Blatov, V. A.; O’Keeffe, M.; Proserpio, D. M. *CrystEngComm* **2010**, 12, 44. (c) Alexandrov, E. V.; Blatov, V. A.; Kochetkova, A. V.; Proserpio, D. M. *CrystEngComm* **2011**, 13, 3947.

(13) Blatov, V. A. *IUCr CompComm Newsletter* **2006**, 7, 4.

(14) The Reticular Chemistry Structure Resource (RCSR) Database: O’Keeffe, M.; Peskov, M. A.; Ramsden, S. J.; Yaghi, O. M. *Acc. Chem. Res.* **2008**, 30, 1782.

(15) (a) Guo, Z.; Wu, H.; Srinivas, G.; Zhou, Y.; Xiang, S.; Chen, Z.; Yang, Y.; Zhou, W.; O’Keeffe, M.; Chen, B. *Angew. Chem., Int. Ed.* **2011**, 50, 3178. (b) Yang, X.-L.; Xie, M.-H.; Zou, C.; Suna, F.-F.; Wu, C.-D. *CrystEngComm* **2011**, 13, 1570. (c) Wen, T.; Li, M.; Zhou, X.-P.; Li, D. *Dalton Trans.* **2011**, 40, 5684. (d) Nouar, F.; Eubank, J. F.; Bousquet, T.; Wojtas, L.; Zaworotko, M. J.; Eddaoudi, M. *J. Am. Chem. Soc.* **2008**, 130, 1833.

(16) For selected recent examples of CPs with the pts topology, see: (a) Caputo, C. B.; Vukotic, V. N.; Sirizzotti, N. M.; Loeb, S. J. *Chem. Commun.* **2011**, 47, 8545. (b) Liu, D.-M.; Xie, Z.-G.; Ma, L.-Q.; Lin, W.-B. *Inorg. Chem.* **2010**, 49, 9107. (c) Davies, R. P.; Less, R.; Lickiss, P. D.; Robertson, K.; White, A. J. P. *Cryst. Growth Des.* **2010**, 10, 4571. (d) Zhang, J.; Xue, Y.-S.; Liang, L.-L.; Ren, S.-B.; Li, Y.-Z.; Du, H.-B.; You, X.-Z. *Inorg. Chem.* **2010**, 49, 7685. (e) Yuan, A.-H.; Lu, R.-Q.; Zhou, H.; Chen, Y.-Y.; Li, Y.-Z. *CrystEngComm* **2010**, 12, 1382. (f) Liang, L.-L.; Zhang, J.; Ren, S.-B.; Ge, G.-W.; Li, Y.-Z.; Du, H.-B.; You, X.-Z. *CrystEngComm* **2010**, 12, 2008. (g) Wu, J.-Y.; Yang, S.-L.; Luo, T.-T.; Liu, Y.-H.; Cheng, Y.-W.; Chen, Y.-F.; Wen, Y.-S.; Lin, L.-G.; Lu, K.-L. *Chem.–Eur. J.* **2008**, 14, 7136.

(17) (a) Kirillova, M. V.; Kirillov, A. M.; Mandelli, D.; Carvalho, W. A.; Pombeiro, A. J. L.; Shul’pin, G. B. *J. Catal.* **2010**, 272, 9. (b) Figiel, P. J.; Kirillov, A. M.; Guedes da Silva, M. F. C.; Lasri, J.; Pombeiro, A. J. L. *Dalton Trans.* **2010**, 39, 9879. (c) Kirillova, M. V.; Kozlov, Y. N.;

Shul'pina, L. S.; Lyakin, O. Y.; Kirillov, A. M.; Talsi, E. P.; Pombeiro, A. J. L.; Shul'pin, G. B. *J. Catal.* **2009**, *268*, 26.

(18) (a) Kirillova, M. V.; Kirillov, A. M.; Kuznetsov, M. L.; Silva, J. A. L.; Fraústo da Silva, J. J. R.; Pombeiro, A. J. L. *Chem. Commun.* **2009**, 2353. (b) Kirillova, M. V.; Kirillov, A. M.; Pombeiro, A. J. L. *Adv. Synth. Catal.* **2009**, *351*, 2936. (c) Kirillova, M. V.; Kirillov, A. M.; Pombeiro, A. J. L. *Chem.–Eur. J.* **2010**, *16*, 9485. (d) Kirillova, M. V.; Kirillov, A. M.; Pombeiro, A. J. L. *Appl. Catal. A: Gen.* **2011**, *401*, 106.

(19) For a recent review on regioselectivity, see: Shul'pin, G. B. *Org. Biomol. Chem.* **2010**, *8*, 4217.

(20) Minisci, F.; Citterio, A.; Giordano, C. *Acc. Chem. Res.* **1983**, *16*, 27.

(21) (a) Kirillova, M. V.; Kuznetsov, M. L.; da Silva, J. A. L.; Guedes da Silva, M. F. C.; Fraústo da Silva, J. J. R.; Pombeiro, A. J. L. *Chem.–Eur. J.* **2008**, *14*, 1828. (b) Kirillova, M. V.; Kuznetsov, M. L.; Reis, P. M.; da Silva, J. A. L.; Fraústo da Silva, J. J. R.; Pombeiro, A. J. L. *J. Am. Chem. Soc.* **2007**, *129*, 10531.

(22) (a) Shilov, A. E.; Shul'pin, G. B. *Activation and Catalytic Reactions of Saturated Hydrocarbons in the Presence of Metal Complexes*; Kluwer Acad. Publ.: Dordrecht, 2000. (b) Olah, G. A.; Molnár, Á. *Hydrocarbon Chemistry*; Wiley: Hoboken, NJ, 2003. (c) Shul'pin, G. B. In *Transition Metals for Organic Synthesis*, 2nd ed.; Beller, M., Bolm, C., Eds.; Wiley-VCH: Weinheim/New York, 2004; Vol. 2, pp 215–242. (d) Olah, G. A.; Surya Prakash, G. K.; Molnár, Á.; Sommer, J. *Superacid Chemistry*, 2nd ed.; Wiley: New York, 2009.

(23) For selected reviews on alkane functionalization, see: (a) Shul'pin, G. B. *Mini-Rev. Org. Chem.* **2009**, *6*, 95. (b) Díaz-Requejo, M. M.; Pérez, P. J. *Chem. Rev.* **2008**, *108*, 3379. (c) Labinger, J. A.; Bercaw, J. E. *Nature* **2002**, *417*, 507. (d) Fokin, A. A.; Schreiner, P. R. *Chem. Rev.* **2002**, *102*, 1551. (e) Sen, A. *Acc. Chem. Res.* **1998**, *31*, 550. (f) Shilov, A. E.; Shul'pin, G. B. *Chem. Rev.* **1997**, *97*, 2879.

(24) Sheldrick, G. M. *Acta Crystallogr.* **2008**, *A64*, 112.